Journal of Renewable Materials

Tech Science Press

DOI: 10.32604/jrm.2022.023371

check for updates

ARTICLE

High Water Resistance and Enhanced Mechanical Properties of Bio-Based Waterborne Polyurethane Enabled by *in-situ* Construction of Interpenetrating Polymer Network

Henghui Deng[1,2], Jingyi Lu[1,2], Dunsheng Liang[1,2], Xiaomin Wang[1,2], Tongyao Wang[1,2], Weihao Zhang[1,2], Jing Wang[3,*] and Chaoqun Zhang[1,2,*]

[1]Key Laboratory for Biobased Materials and Energy of Ministry of Education, College of Materials and Energy, South China Agricultural University, Guangzhou, 510642, China

[2]Guangdong Laboratory for Lingnan Modern Agriculture, Guangzhou, 510642, China

[3]Guangdong Provincial Key Laboratory of Silviculture, Protection and Utilization, Guangdong Academy of Forestry, Guangzhou, 510520, China

[*]Corresponding Authors: Chaoqun Zhang. Email: zhangcq@scau.edu.cn; nwpuzcq@gmail.com; Jing Wang. Email: wangjingmos@hotmail.com

Received: 22 April 2022 Accepted: 06 May 2022

ABSTRACT

In this study, acrylic acid was used as a neutralizer to prepare bio-based WPU with an interpenetrating polymer network structure by thermally induced free radical emulsion polymerization. The effects of the content of acrylic acid on the properties of the resulting waterborne polyurethane-poly (acrylic acid) (WPU-PAA) dispersion and the films were systematically investigated. The results showed that the cross-linking density of the interpenetrating network polymers was increased and the interlocking structure of the soft and hard phase dislocations in the molecular segments of the double networks was tailored with increasing the content of acrylic acid, leading to enhancement of the mechanical properties and water resistance of WPU-PAA films. Notably, with the increase in content of acrylic acid, the tensile strength, Young's modulus, and toughness of the WPU-PAA-110 film increased by 3 times, and 8 times, and 2.4 times compared with WPU-PAA-80, respectively. The WPU-PAA-100 film showed the best water resistance, and the water absorption rate at 96 h was only 3.27%. This work provided a new design scheme for constructing bio-based WPU materials with excellent properties.

KEYWORDS

Bio-based waterborne polyurethane; interpenetrating polymer network; highly water resistance; superior mechanical performance

1 Introduction

Waterborne polyurethanes (WPU) have become one of the most important environmental-friendly polymers and have been widely used in various applications ranging from leather finishing agents, coatings, and adhesives due to their advantages such as low volatile organic compounds (VOCs), abrasion resistance, flexibility, and resilience [1–3]. Recently, the application of renewable resources as a replacement of fossil feed stock to develop bio-based chemicals (such as polyols, isocyanates and

hydrophilic chain extenders, etc.) and therefrom endow the sustainability and green characteristics of the final products of WPU [4].

Among them, vegetable oils are one of the most promising renewable resources for the production of bio-based WPU due to the advantages of low cost and abundant availability [5]. In addition, the existing active sites of vegetable oils (carbon-carbon double bonds, ester groups, etc.) provide an effective platform for the preparation of value-added chemicals required for the synthesis of bio-based WPU. For example, Wang et al. [6] synthesized a novel oleic-based primary glycol via Claisen condensation and thiol-ene photo-click reactions on the ester bond and carbon-carbon double bond of methyl oleate and used it as a substitute for petroleum-based diol to prepare bio-based WPU. Omrani et al. [7] prepared a new type of carboxylic acid group-containing polyol through epoxy ring-opening and saponification of the carbon-carbon double bond and triglyceride bond of sunflower oil, respectively, which was further used as a hydrophilic chain extender to prepare biodegradable bio-based WPU. Fu et al. [8] developed a new linear saturated terminal diisocyanate by thiol-ene coupling and Curtius rearrangement of the carbon-carbon double bond and carboxyl group of castor oil-derived undecylenic acid and further reacted with castor oil-derived polyol and hydrophilic chain extender to prepare a fully bio-based WPU.

Generally, neutralizer is indispensable for the preparation of WPU and is applied for the dispersion of the WPU in the water. Although used in very small amounts, more and more attention has been attracted to exploring green neutralizers and simultaneously tailoring the performance of the resulting bio-based WPU. For example, Gurunathan et al. [9] obtained a cationic castor oil-based WPU with a solid content of 30% with hydrochloric acid as a neutralizer for neutralizing the methyldiethanolamine and polyaniline in the molecular chain of castor oil-based polyurethane. Zhi et al. [10] prepared a series of cationic castor oil-based WPU with different solid contents with acetic acid as a neutralizer, and further infiltrated the obtained WPU into three types of rift-cut wood veneers through a vacuum impregnation process to develop flexible decorative veneers. As the acetic acid content in the WPU increased, the degree of protonation of the tertiary amine group of methyldiethanolamine in WPU improved, leading to the increased content of WPU adsorption in the wood caplets during impregnation. Liang et al. [11] developed a series of cationic castor oil-based WPU with UV absorption, anticorrosion properties, and long-term antibacterial performance with glutamic acid and aspartic acid as neutralizers. It is found amino acids not only acted as neutralizers, but also functioned as a hydrogen bond donors and hydrogen bond acceptors, leading to a significant improvement in the performance of the WPU films. Zhang et al. [12] prepared a series of cationic castor oil-based WPU films with high ultraviolet absorption and antibacterial properties using several natural phenolic acids (caffeic acid, ferulic acid, syringic acid, gallic acid, and salicylic acid) as functional neutralizers. These natural phenolic acids not only function as neutralizers in polymers, but also bridge the soft and hard segments of WPU through hydrogen bonds, significantly optimizing the performance of bio-based WPU.

Acrylic acid, as a typical type of organic acid with a simple molecular structure (carboxyl group and conjugated double bond, etc.), could be used as a potential neutralizer for cationic bio-based WPU. In this work, acrylic acid was introduced as a new neutralizer into bio-based WPU prepared from castor oil to facilitate the dispersion of WPU into water, and further obtained bio-based waterborne polyurethane-poly (acrylic acid) (WPU-PAA) dispersions with an interpenetrating polymer network via thermally induced free radical emulsion polymerization. According to this strategy, a series of cationic bio-based WPU-PAA with an interpenetrating polymer network was prepared and characterized. The particle size and stability of interpenetrating polymer network structural dispersions prepared with different contents of neutralizer were systematically studied. The properties of interpenetrating polymer films, including gel content, thermomechanical properties, thermal stability, surface water contact angle, mechanical properties, coating properties and water resistance were systematically analyzed. This work provided a

new idea for compositional control and structural design strategies to modulate bio-based WPU with comprehensive excellent properties.

2 Materials and Methods

2.1 Materials

Castor oil (hydroxyl value: 164 mg KOH g^{-1}) was provided by Tianjin Fuyu Reagent Company (China). Isophorone diisocyanate (IPDI) and methyldiethanolamine (MDEA) were purchased from Guangdong Wengjiang Chemical Reagents Co., Ltd. (China). Acrylic acid and 2,2′-Azobis(2-methylpropionitrile) (AIBN) were obtained from Shanghai Aladdin Biochemical Reagent Technology Co., Ltd. (China). Dibutyltin dilaurate (DBTDL) was purchased from Fuchen Reagent Factory. Methyl ethyl ketone (MEK) was purchased from Hongda Chemical Co., Ltd. (China). Deionized water was prepared in the laboratory. All chemical reagents were used directly after purchase.

2.2 Methods

2.2.1 Synthesis of Cationic Bio-Based WPU Dispersions from Acrylic Acid

A series of bio-based WPU dispersions were prepared in a molar ratio of 1:2:0.99 of OH (from castor oil):NCO (from IPDI):OH (from MDEA). The typical WPU dispersions preparation route was shown in Scheme 1, and the detailed preparation process was as follows. First, castor oil and IPDI were mixed homogeneously in a double-neck round-bottom flask with stirring (190–210 rpm) for 10 min at 78°C. Then, the DBTDL (20 μL) was added to the double -necked round-bottom flask to facilitate the synthesis of the prepolymer, which was kept stirring for 10 min. After that, the MDEA was added to the prepolymer for polymerization to further achieve the growth of the polyurethane polymer chain. When the prepolymer was reacted to a completely immobile state, 30 mL of MEK was added to the double-neck round-bottom flask to reduce the viscosity of the prepolymer, and the reaction was continued in the solution for 2 h. Subsequently, the solution was cooled to room temperature, and the acrylic acid was added to neutralize the MDEA to increase the hydrophilicity of the polymer chain. The content of acrylic acid was determined according to the molar ratio of carboxyl groups in acrylic acid to tertiary amine groups in MDEA, which were 80%, 90%, 100%, and 110% of the molar ratio of tertiary amine groups in MDEA, respectively. Finally, the deionized water was added to the prepolymer solution under vigorous stirring to form WPU dispersions. The WPU dispersions with a solids content of 25 wt.% was obtained by rotary evaporation of MEK.

2.2.2 Synthesis of WPU-PAA Dispersions

A series of WPU dispersions with different contents of acrylic acid were further prepared WPU-PAA dispersions through free radical emulsion polymerization radical reaction with acrylic acid. These WPU dispersions were reacted at 80°C for 3 h with the AIBN dissolved in ethanol as a thermal initiator to form an interpenetrating polymer network. The obtained WPU-PAA dispersions were named as WPU-PAA-80, WPU-PAA-90, WPU-PAA-100, and WPU-PAA-110 according to the content of acrylic acid, respectively. The reaction route of the WPU-PAA dispersions was shown in Scheme 1.

2.2.3 Synthesis of WPU-PAA Films

In order to further analyze the properties of WPU-PAA films with an interpenetrating polymer network structure, the WPU-PAA dispersions (15 mL) were poured into a siliconized glass dish with a diameter of 60 mm and air-dried to form films. After the surface of all the films was dried, it was moved into a 60°C vacuum oven for 24 h to evaporate the remaining moisture.

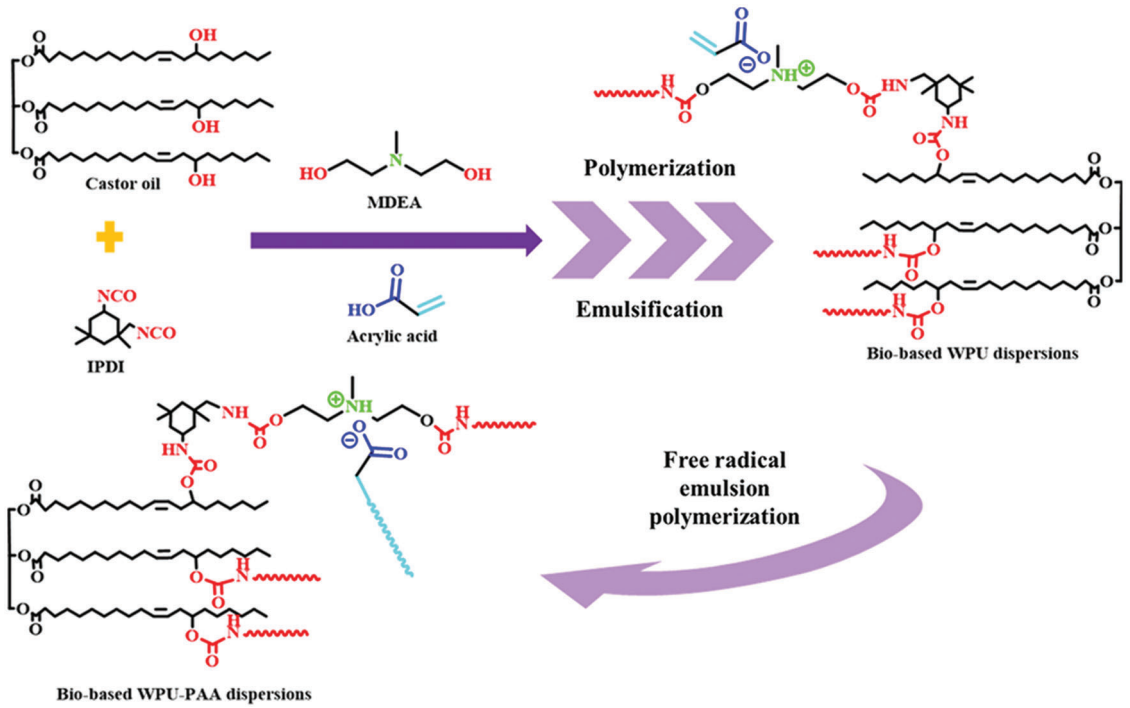

Scheme 1: The synthetic route of the WPU and the WPU-PAA dispersions

2.3 Characterization

The particle size and Zeta potential of the WPU-PAA dispersions were measured by a Zeta-sizer Nano ZSE (Malvern Instruments). The WPU-PAA dispersions were diluted with distilled water to about 0.01 wt.% before the test. The storage stability of all WPU-PAA dispersions was evaluated by centrifuging the dispersions on Tomos 3–18 to 8000 rpm for 60 min.

The degree of crosslinking of the WPU-PAA films was determined by the gel content. The gel content was obtained from the calculated mass loss after soaking the films in tetrahydrofuran (THF) for 24 h. The calculation formula was as follows:

$$\text{Gel content } (\%) = \frac{m_2}{m_1} \times 100\% \quad (1)$$

where "m_1" was the dry weight of the initial sample, and "m_2" was the dry weight of the sample after soaking in THF for 24 h. The gel content value of the samples was the average value of four parallel samples. The error bars were from the standard error of the results of four parallel samples.

The Netzsch DMA 242C dynamic mechanical analyzer was used to analyze the dynamic mechanical behavior of the obtained films. The films were made into elongated specimens (length: 0.5 cm, width: 2 cm) and heated from –60°C to 100°C at a heating rate of 5 °C min^{-1}, and the stretching frequency was maintained at 1 Hz throughout the heating process. The highest peak of the loss factor curve was considered to be the T_g of the films.

Thermogravimetric analysis (TGA) of the resulting films was performed on a discovery TGA-550 thermal analyzer. The film samples were heated from 30°C to 700°C at a heating rate of 10 °C min^{-1} in a nitrogen-protected atmosphere.

The contact angle goniometer (Powereach JC2000C1) was used to investigate the water contact angle of the films surface by the static drop method. Each sample was repeated more than 5 times, and the average value was obtained. The error bars were from the standard error of the results of five parallel tests.

The mechanical properties of the resulting films were determined by tensile testing. Tensile tests (crosshead speed: 100 mm min^{-1}) of all samples were carried out on an electronic universal testing machine (UTM-4204). All samples were subjected to 3 parallel tests and the average value was obtained; the error bars were from the standard error of the results of 3 parallel tests. All samples were cut into long strips (length: 4 cm, width: 1 cm).

The pencil hardness and the horizontal texture adhesion of WPU-PAA films were evaluated by ASTM D-3363 and ASTM D-3359. The samples were prepared by casting 1 mL of the WPU-PAA dispersions on a 5 × 10 cm^2 tinplate and vacuum drying.

The water resistance of the films was evaluated by the immersing method. All samples (4 parallels) were made into 10 mm^2 squares and dried at 60°C for 12 h before testing, and the dried samples were immersed in water for 96 h. The ratio of the mass of the soaked sample to the initial mass was calculated as the water absorption rate of the sample. The calculation formula was as follows:

$$W\% = \frac{W_1 - W_0}{W_0} \tag{2}$$

where W_0 and W_1 were the weight of the films before testing and after absorbing water. The higher the water absorption rate, the worse the water resistance of the films.

3 Results and Discussion

Generally, inorganic acid (hydrochloric acid) and organic acids (acetic acid, natural phenolic acid, and amino acid, etc.) were widely used to neutralize tertiary amines for the dispersion of cationic waterborne WPU. Several research groups have been devoted to exploring other acids to tailor the performance of the resulting cationic waterborne WPU [11,12]. Acrylic acid is an industrial raw material with a simple structure containing one carboxyl group and one conjugated double bond. This acid could be used not only as a neutralizer for cationic bio-based WPU, but also for thermally induced free radical emulsion polymerization for *in-situ* constructing of interpenetrating poly(acrylic acid) network [13,14], which was applied to enhance the final performance (such as mechanical properties, water resistance) of the resulting cationic bio-based WPU.

3.1 Preparation and Characterization of WPU-PAA Dispersions

The WPU-PAA dispersions were prepared by the polyaddition between castor oil and IPDI with MDEA as the hydrophilic chain extender and acrylic acid as the neutralizer followed by the thermally induced free radical emulsion polymerization of acrylic acid.

The appearance, particle size, and Zeta potential of these dispersions were shown in Figs. 1a and 1b, and Table 1. In general, Zeta potential is an important property in the study of polymer dispersions, which is related to the stability of dispersions. As shown in Table 1, the Zeta potential of the WPU-PAA dispersions increased with the increasing content of acrylic acid, indicating that the increased degree of the tertiary amine groups of the MDEA fragments in the polymer were protonated by the carboxyl groups in the acrylic acid, leading to an increase in the positively charged sites of the resulting WPU-PAA. The highest Zeta potential of WPU-PAA-100 was 65.5 mV, and the amine groups in MDEA segments were completely neutralized by the carboxyl groups of acrylic acid. When the content of acrylic acid was further increased, the Zeta potential of WPU-PAA-110 did not continue to increase and the excess acrylic acid was dissolved in the aqueous phase.

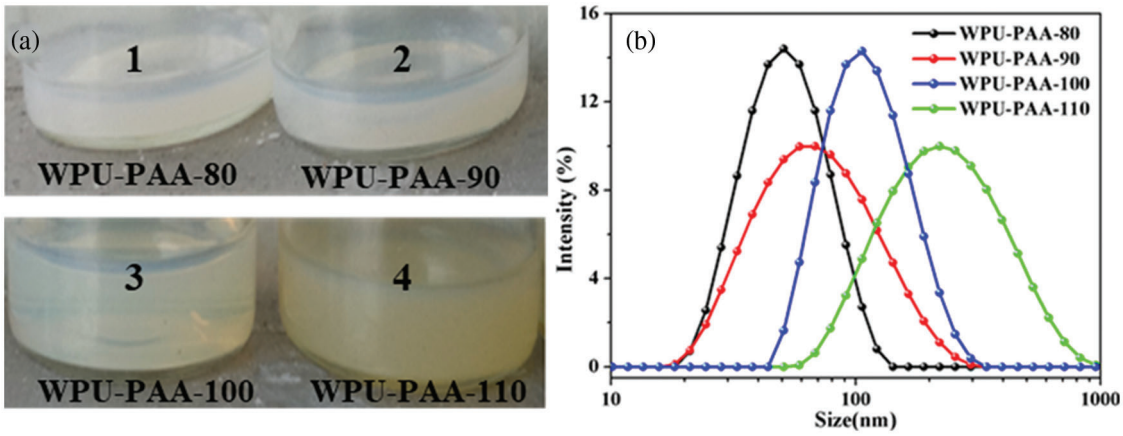

Figure 1: (a) Appearance of WPU-PAA dispersions. (b) Particle size distribution curves of WPU-PAA dispersions

Table 1: Properties of WPU-PAA dispersions

Samples	pH values	Appearance	Z-average size (nm)	Zeta potential (mV)	Storage life
WPU-PAA-80	4.13	Transparent	51.05 ± 1.38	45.6 ± 0.43	>2 years
WPU-PAA-90	3.85	Transparent	64.44 ± 4.56	50.3 ± 0.52	>2 years
WPU-PAA-100	3.67	Transparent	103.57 ± 3.47	65.5 ± 0.14	>2 years
WPU-PAA-110	3.49	Translucent	220.47 ± 5.12	64.2 ± 0.37	>2 years

The appearance of these WPU-PAA dispersions (see Fig. 1a) changed from a transparent state to a translucent state with the increasing content of acrylic acid, which was correlated with the particle size of the dispersions. Among them, the particle size of WPU-PAA-80, WPU-PAA-90, WPU-PAA-100, and WPU-PAA-110 was 51.05, 64.44, 103.57, and 220.47 nm, respectively, indicating that the particle size of these dispersions increased with the increasing content of acrylic acid. As mentioned earlier, the increased degree of protonation of the tertiary amine groups of the MDEA fragments in WPU-PAA would lead to an increase in the hydrophilicity of the polymer and thus reduce the particle size of the dispersions. However, in addition to the content of the hydrophilic group, other factors, such as soft/hard segment contents, crosslinking densities, and so on, also affect the particle size of the dispersion [15]. Here, the particle size of the WPU-PAA dispersions was related to another important group conjugated double bond in acrylic acid. As the content of acrylic acid increased, the content of conjugated double bonds also increased and underwent a free radical emulsion polymerization under thermally induced conditions, which further crosslinked the dispersion and increased the crosslinking densities of WPU-PAA, resulting in an increase in the particle size of the dispersion [16].

To further evaluate the stability of the dispersions, all WPU-PAA dispersions were centrifuged at 8000 rpm for 60 min. The results indicated that all the samples did not precipitate, indicating the excellent storage stability of these dispersions. In addition, all dispersions were stored in the laboratory environment for more than two years without any precipitation.

3.2 Preparation and Characterization of WPU-PAA Films

The WPU-PAA films were prepared by the evaporation of the water of the dispersions at 60°C in a vacuum oven. These films were characterized by gel content testing, DMA, DSC, TGA, and tensile testing.

The gel content testing was generally used to qualitatively measure the crosslinking degree of the polymer films [17]. In this study, two factors would affect the gel content of the resulting WPU-PAA films: i) whether the active groups of IPDI with castor oil and MDEA were completely consumed; ii)

whether the poly (acrylic acid) network formed by the thermally initiated radical reaction had a structural complementary effect with the WPU network. After being soaked in THF for 24 h as shown in Fig. 2a and Table 2, the gel contents of WPU-PAA-80, WPU-PAA-90, WPU-PAA-100, and WPU-PAA-110 were 90.54%, 93.87%, 95.36%, and 97.43%, respectively, indicating the high cross-linking degree of WPU-PAA films with an interpenetrating polymer network structure. Based on the above results, the following statement could be concluded: i) castor oil and MDEA almost completely reacted with IPDI, resulting in a 3-D crosslinking polymer network [18]. ii) After polymerization of acrylic acid, interpenetrating polymer networks containing WPU and poly(acrylic acid) were *in-situ* constructed through strong ionic bonds and topological interlocking effect, resulting in the formation of the dense, orderly and tightly polymer structure and therefore the hindrance of THF penetration into the films [19].

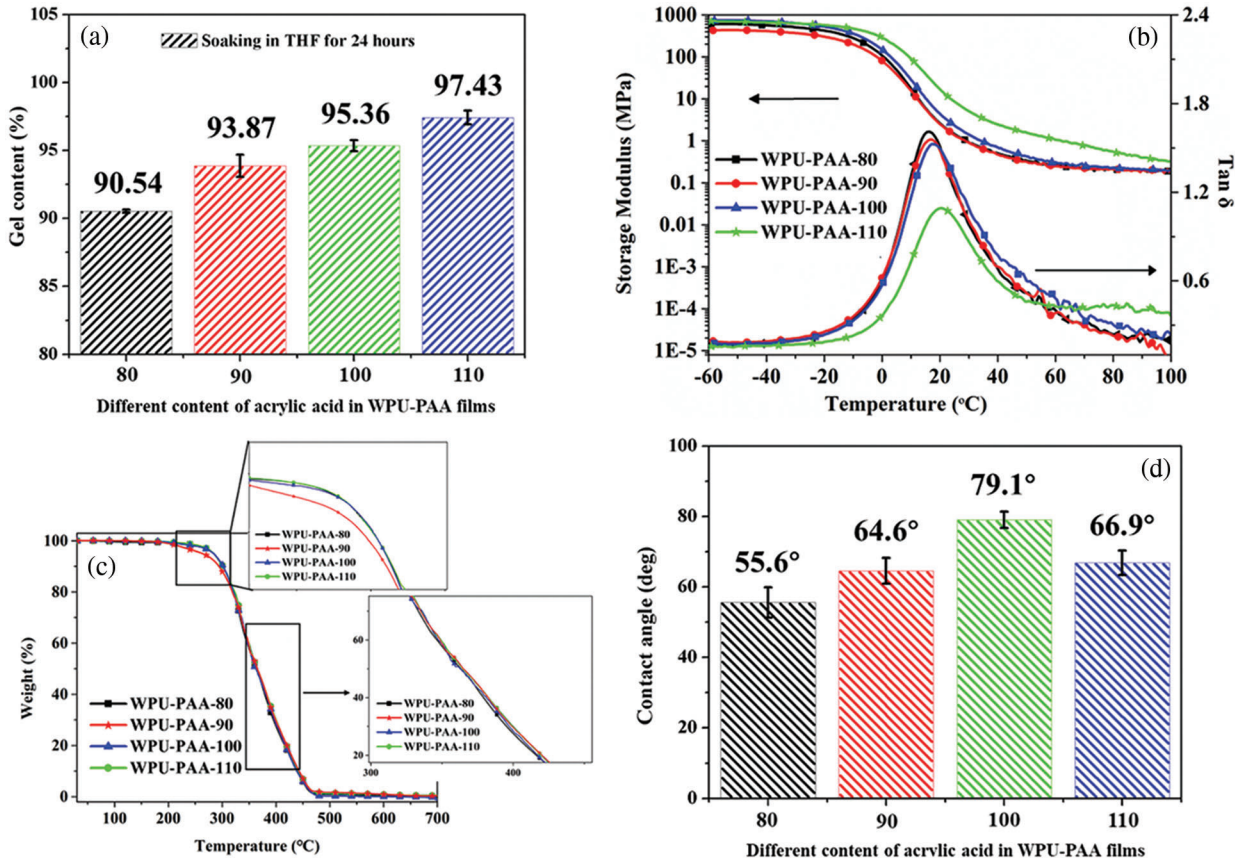

Figure 2: (a) Gel content of WPU-PAA films after soaking in THF for 24 h. (b) Storage modulus and loss factor curves of WPU-PAA thin films. (c) TGA curves of WPU-PAA films. (d) Water contact angle on the surface of WPU-PAA films

Table 2: DMA and TGA data of WPU-PAA films

Samples	DMA			TGA		
	T_g (°C)	E' at 25°C (MPa)	v_e (mol/m^3)	T_5 (°C)	T_{50} (°C)	T_{max} (°C)
WPU-PAA-80	16.37	1.43	48.43	284.27	363.37	335.07
WPU-PAA-90	16.95	1.61	49.04	284.47	364.77	352.37
WPU-PAA-100	17.30	2.53	61.88	284.17	362.77	353.27
WPU-PAA-110	20.33	8.71	192.23	263.67	364.97	351.17

In order to further quantitatively analyze the cross-linking density (v_e), storage modulus (E') and glass transition temperature (T_g) of WPU-PAA polymers. The detailed data of DMA measurement were shown in Fig. 2b and Table 2. The v_e of the WPU-PAA films were calculated with the formula as shown below according to the method reported previously [20]

$$E' = 3\, v_e\, R\, T \tag{3}$$

where R represented the universal gas constant with a value of 8.314 J mol^{-1} K^{-1}, $T = T_g + 30^oC$, and E' was the storage modulus corresponding to T.

As seen in Table 2, the v_e of the resulting WPU-PAA films increased with the increasing content of acrylic acid. The calculated v_e of WPU-PAA-80 and WPU-PAA-110 were 48.43 mol m^{-3} and 192.23 mol m^{-3}, respectively. The v_e of WPU-PAA-110 was about 4 times that of WPU-PAA-80 due to the higher crosslinked structure induced by the radical polymerization of more acrylic acid in WPU-PAA-110 [21]. In addition, large amounts of hydrogen bonding between WPU and poly(acrylic acid) also attributed to the increase in the physically crosslinking of the interpenetrating polymer network: i) The formation of close-packed hydrogen bonds between carboxyl groups [22]; ii) The formation of free hydrogen bonds between carboxyl groups and the urethane bond [23]; iii) The formation of free hydrogen bonds between urethane bonds [24].

Fig. 2b shows the E' and tan δ of WPU-PAA in the temperature range from –60°C to 100°C. All polymer films exhibited a glassy state when the temperature was below –20°C, and the E' of these films exhibited a similar slight decreasing trend from –60°C to –20°C. As the temperature increased to 60°C, the E' of WPU-PAA films rapidly decreased by three orders of magnitude, which was related to the relaxation process of the polymer segments. In this temperature range, the largest peak of the tan δ curve of the WPU-PAA films could be observed, which was considered to be the T_g of the WPU-PAA films. Obviously, these films exhibited only one peak in the tan δ curve due to their homogeneous properties. When the temperature continued to rise above 60°C, the WPU-PAA polymers exhibited rubbery properties, and the E' of the curves showed a plateau stage. Here, the E' and T_g of WPU-PAA improved with the addition of acrylic acid. The WPU-PAA-110 film exhibited the highest E' of 8.71 MPa and the highest T_g of 20.33°C, and the WPU-PAA-80 film exhibited the lowest E' of 1.43 MPa and the lowest T_g of 16.37°C. The variation of these two properties could be explained by the difference in v_e of these two polymers. Considering WPU-PAA-110 film had a high v_e, the space gap inside the material was small, and the movement of molecular chains was hindered, leading to the difficulty of the elastic deformation of the polymer and therefore the highest E' [17]. At the same time, a higher temperature was required to transform the polymer material from a glassy to rubbery a state, resulting in the highest T_g of WPU-PAA-110 [25].

Fig. 2c showed the TGA curve of the WPU-PAA films to analyze their thermal stability. The T_5, T_{10}, T_{max} (the temperature corresponding to the mass loss of the polymer material was 5%, 10%, and the maximum degradation mass, respectively) of WPU-PAA films were summarized in Table 2. The thermal stability of WPU-PAA films was related to the flexible network (WPU) and the rigid network (poly (acrylic acid)), as well as the interpenetration structure of the double network. It could be observed from Fig. 2c that all WPU-PAA films undergo three thermal degradation stages. First, the thermal degradation of the films at 250°C–320°C could be attributed to the decomposition of the rigid poly(acrylic acid) network and unstable urethane bonds in the materials, formed small molecules such as CO and olefins [26]. At this stage, the thermal stability of WPU-PAA-110 was the worst, and the mass loss of the thermal degradation process was the largest compared to other WPU-PAA films. This was due to the fact that the acrylic acid content in WPU-PAA-110 was the highest, forming a dense and rigid network of poly(acrylic acid), resulting in the dissociation of the molecular chains in the polymer due to poor thermal mobility [27]. The second stage was the fastest thermal degradation process of the WPU-PAA films, which was mainly the degradation of the unsaturated fatty acid chains of castor oil in the flexible

network of WPU and the residual interpenetrating polymer network structure in the temperature range of 320°C–420°C [20]. During this thermal degradation stage, there was no obvious difference in the degradation behavior of the WPU-PAA films due to the same castor oil content used to prepare the polymers. Finally, the third-stage thermal degradation process of the WPU-PAA film occurred above 420°C, corresponding to the decomposition of residual components [20].

Fig. 2d showed the water contact angle of the WPU-PAA films. It could be observed that the surface of the WPU-PAA films with the interpenetrating polymer network structure generally tended to be hydrophilic due to the presence of ionic groups, and the contact angles of the films were all less than 90°. In detail, with the increasing content of acrylic acid, the surface water contact angle of the WPU-PAA films first increased and then decreased. The surface water contact angles of the films of WPU-PAA-80, WPU-PAA-90, WPU-PAA-100 and WPU-PAA-110 were 55.6°, 64.6°, 79.1°, and 66.9°, respectively. There were three factors that affected the surface water contact angle of WPU-PAA films, including the degree to which the tertiary amine groups of MDEA in the polymer were protonated, the v_e of the interpenetrating polymer network of the WPU-PAA, and the content of acrylic acid did not participate in neutralizing MDEA [28]. In theory, as the content of acrylic acid increased, the surface hydrophilicity of the films improved with increasing the degree of protonation of the tertiary amine groups of MDEA in the polymer, resulting in a reduction in the surface water contact angle of the films. Apart from the surface hydrophilicity, the surface water contact angle of the films was also affected by the interpenetrating polymer network. With the increase of content of acrylic acid, increasing the v_e of the interpenetrating polymer network of WPU-PAA, resulting in the formation of a dense poly (acrylic acid) network that shielded the hydrophilic groups of the surface of the films. The influence of hydrophilic groups on the surface water contact angle of the films was eliminated. Therefore, the surface water contact angle of the film of the WPU-PAA-100 was 23.5° higher than that of the WPU-PAA-80. However, the WPU-PAA-100 film still showed a hydrophilic surface due to the high content of hydrophilic groups in the polymer, resulting in a water contact angle below 80°. In addition, the acrylic acid that did not participate in the neutralization of MDEA was still grafted to the polyacrylic acid network to improve the hydrophilicity of the film surface, leading to a decrease in the surface contact angle of the films. Therefore, the surface water contact angle of the films of WPU-PAA-110 was reduced compared with that of WPU-PAA-100.

In order to further investigate the effect of the content of acrylic acid on the mechanical properties of WPU-PAA films, all WPU-PAA films were tested for mechanical properties on an electronic universal testing machine. Detailed mechanical property data including tensile strength, elongation at break, Young's modulus, and toughness were summarized in Figs. 3a–3c and in Table 3. Fig. 3c showed the stress-strain curves of a series of WPU-PAA films. It could be observed that the tensile strength of the WPU-PAA films improved with increasing the content of acrylic acid. In detail, as the content of acrylic acid increased, the tensile strength of the WPU-PAA-110 film was increased to 6.21 MPa, which was 3 times that of the WPU-PAA-80 film. This could be attributed to the large difference in the v_e of the interpenetrating polymer network between WPU-PAA-110 and WPU-PAA-80. In addition, with an increase in the content of acrylic acid, the ordered arrangement of soft phase and hard phase dislocations in the interlocking structure of the double network was tailored [29], and the content of ionic bonds between WPU and Poly(acrylic acid) increased in the WPU-PAA films [30], resulting in a significant improvement in the tensile strength of the WPU-PAA-110 film. The elongation at break of WPU-PAA-80 was 614.15%, meaning that the WPU-PAA-80 film could be stretched more than 6 times its own length. Although the elongation at break of WPU-PAA films was decreased with increasing the content of acrylic acid, the elongation at break of WPU-PAA-110 could still be maintained at around 200%. This could be attributed to the flexible fatty acid chain properties of castor oil in the WPU-PAA films. Figs. 3a and 3b showed the trend of Young's modulus and toughness improvement of the WPU-PAA films with increasing the content of acrylic acid. The improvement of these two important properties of the polymer

materials, in addition to the above-mentioned factors (the ionic bonding force between WPU and poly(acrylic acid), the v_e of the film, and the interlocking structural arrangement of the double network), the internal hydrogen bond content of polymers played a key role [31]. When the WPU-PAA films were stimulated by external force, the strong and dense hydrogen bonds inside the polymer were sacrificed to dissipate energy, resulting in an increase in the Young's modulus and toughness of the WPU-PAA films [32].

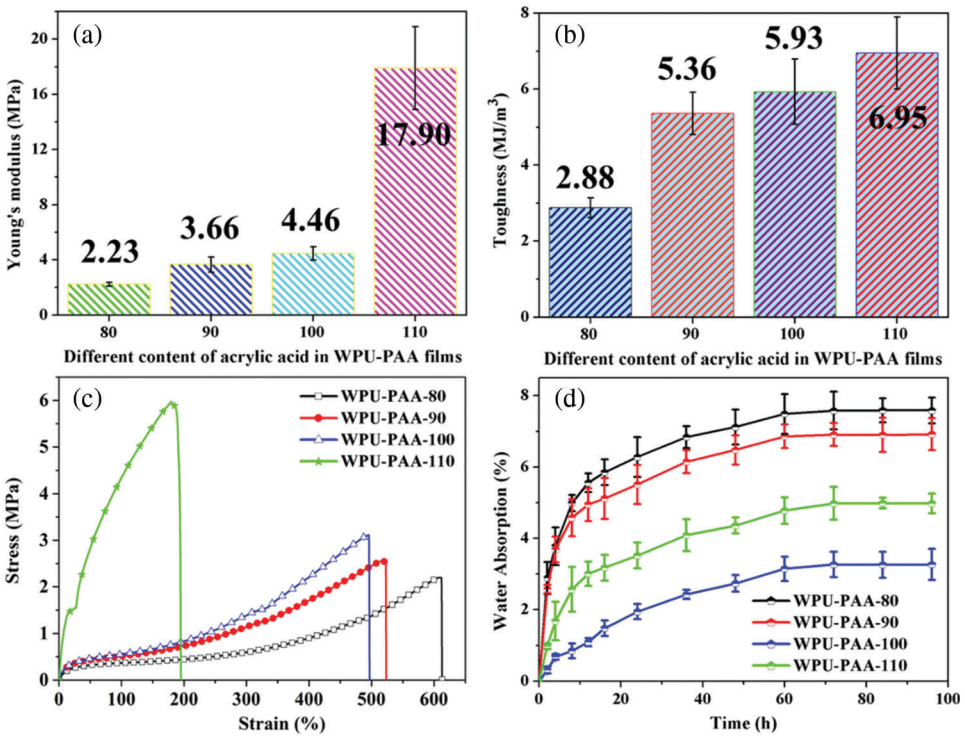

Figure 3: Young's modulus (a), Toughness (b), Stress-strain curve (c), and water absorption (d) of WPU-PAA films

Table 3: Mechanical properties, Water absorption, Pencil hardness and Crosshatch adhesion data of WPU-PAA films

Samples	Tensile strength (MPa)	Elongation at break (%)	Young's modulus (MPa)	Toughness (MJ/m^3)	Water absorption at 96 h (%)	Pencil hardness (3B-HB-3H, 3H = best)	Crosshatch adhesion (5B = best)
WPU-PAA-80	2.07 ± 0.09	614.15 ± 12.73	2.23 ± 0.15	2.88 ± 0.26	7.58	2B	2B
WPU-PAA-90	2.59 ± 0.34	525.53 ± 18.53	3.66 ± 0.99	5.36 ± 0.56	6.92	1H	2B
WPU-PAA-100	3.08 ± 0.31	460.67 ± 49.63	4.46 ± 0.49	5.93 ± 0.86	3.27	2H	4B
WPU-PAA-110	6.21 ± 0.02	196.76 ± 18.57	17.90 ± 3.01	6.95 ± 0.95	4.98	3H	5B

The coating properties of the resulting WPU-PAA films, including data on pencil hardness and crosshatch adhesion, were summarized in Table 3. The results showed that the pencil hardness and crosshatch adhesion of a series of WPU-PAA films were improved with the increase of the content in acrylic acid. The pencil hardness of the films of WPU-PAA-110 and WPU-PAA-80 was 3H and 2B,

respectively. This was attributed to increasing the hard segment content of poly(acrylic acid) in the polymer [33]. All WPU-PAA samples exhibited excellent crosshatch adhesion, which increased from 2B to 5B with increasing the content of acrylic acid. The content of polar groups (ester groups, carboxyl groups, urethane bonds) in the coating increased with increasing the content of acrylic acid, resulting in enhanced crosshatch adhesion between the coating and the substrate [25,34].

The water resistance of a series of WPU-PAA films was further evaluated by the immersion method. The detailed data of the water absorption of the films (within 96 h) were collated in Fig. 3d and Table 3. As shown in Fig. 3d, the water absorption process of the films was divided into three stages: fast absorption, slow absorption, and absorption equilibrium. The water absorption rate of the samples increased rapidly within 12 h after being immersed in deionized water. In the time range of 12–60 h, the water absorption of the samples showed a slow upward trend. Finally, after immersion in deionized water of the films for 60 h, the samples reached the absorption equilibrium, and the water absorption rate only slightly changed up and down. The test results of the water absorption of WPU-PAA films showed that with the increase in content of acrylic acid, the water absorption of WPU-PAA films at the time of absorption equilibrium showed a trend of first decreasing and then increasing. Among them, WPU-PAA-100 exhibited the lowest water absorption rate of 3.27%, indicating that WPU-PAA-100 had the best water resistance. This could be explained by the high v_e of the interpenetrating polymer network structure and the shielding effect of the poly(acrylic acid) network on the hydrophilic groups, which hindered the entry of water into the film interior [35]. The water absorption of the films of the WPU-PAA-110 was improved compared to the WPU-PAA-100, which was due to the fact that the acrylic acid not involved in neutralization of MDEA was grafted into the polyacrylic acid network, improved the hydrophilicity of the polymer, leading to an increase in the water absorption of the WPU-PAA-110 film [36].

In Table 4, the appearance, particle size, tensile strength, pencil hardness, and water absorption of WPU-PAA were compared with the reported work. In the comparative work, the preparation method of PU164-0.99 was almost the same as the synthesis steps except that the neutralizing agent used was acetic acid. The comparison found that the tensile strength and water absorption performance of the WPU-PAA sample with an interpenetrating polymer network were better than PU164-0.99, which could explain from another perspective that the formation of the interpenetrating network in WPU-PAA was beneficial to improving the polymerization tensile strength and water absorption. The appearance of PU-164-0.99 was translucent and yellowish, and the particle size was 25.8 nm smaller than that of WPU-PAA dispersion, which was caused by the hydrophilic nature and single network structure of PU-164-0.99.

Table 4: The properties of WPU-PAA and comparison with WPU reported in literature

Sample	Appearance	Z-average size (nm)	Tensile strength (MPa)	Pencil hardness	Water absorption at 96 h (%)
WPU-PAA-80	Transparent	51.05 ± 1.38	2.07 ± 0.09	2B	7.58
WPU-PAA-90	Transparent	64.44 ± 4.56	2.59 ± 0.34	1H	6.92
WPU-PAA-100	Transparent	103.57 ± 3.47	3.08 ± 0.31	2H	3.27
WPU-PAA-110	Translucent	220.47 ± 5.12	6.21 ± 0.02	3H	4.98
PU164-0.99 [37]	Translucent with yellow light	25.8	0.93 ± 0.09	–	7.97 ± 0.17[a]

Note: [a]the value corresponding to the water absorption after 20 d immersion.

4 Conclusions

In this work, a series of cationic bio-based WPU-PAA with an interpenetrating polymer network structure were successfully prepared by radical polymerization of acrylic acid neutralizer. The effects of the content of acrylic acid on WPU-PAA dispersions and films were systematically investigated. The results showed that the Zeta potential and particle size of the dispersion increased with increasing the content of acrylic acid. With the increase in content of acrylic acid, the crosslinking densities of the interpenetrating polymer networks improved and the interlocking structure of soft-phase and hard-phase dislocations arrangements was tailored, resulting in the increase of gel content, E', T_g, pencil hardness, and crosshatch adhesion of WPU-PAA films. As the content of acrylic acid increased, the tensile strength, Young's modulus, and toughness of the WPU-PAA-110 film were increased by 3 times, 8 times, and 2.4 times that of the WPU-PAA-80 film, respectively. More notably, the water absorption of the WPU-PAA-100 film within 96 h was only 3.27%, indicating that the interpenetrating polymer network structure effectively improved the water resistance of the films. This work provided a simple and effective method for the design of bio-based polymers with high water resistance and mechanical robustness.

Funding Statement: This work was sponsored by the Research and Development Program in Key Areas of Guangdong Province (Grant No. 2020B0202010008), Guangdong Province Science & Technology Program (2018B030306016), Guangdong Provincial Innovation Team for General Key Technologies in Modern Agricultural Industry (2019KJ133), Key Projects of Basic Research and Applied Basic Research of the Higher Education Institutions of Guangdong Province (2018KZDXM014).

Conflicts of Interest: The authors declare that they have no conflicts of interest to report regarding the present study.

References

1. Kang, S. Y., Ji, Z., Tseng, L. F., Turner, S. A., Villanueva, D. A. et al. (2018). Design and synthesis of waterborne polyurethanes. *Advanced Materials, 30(18),* e1706237. DOI 10.1002/adma.201706237.
2. Wang, D., Wang, Z., Ren, S., Xu, J., Wang, C. et al. (2021). Molecular engineering of colorless, extremely tough, superiorly self-recoverable, and healable poly(urethane-urea) elastomer for impact-resistant applications. *Materials Horizons, 8(8),* 2238–2250. DOI 10.1039/D1MH00548K.
3. Ghasemlou, M., Daver, F., Ivanova, E. P., Murdoch, B. J., Adhikari, B. (2020). Use of synergistic interactions to fabricate transparent and mechanically robust nanohybrids based on starch, non-isocyanate polyurethanes, and cellulose nanocrystals. *ACS Applied Materials & Interfaces, 12(42),* 47865–47878. DOI 10.1021/acsami.0c14525.
4. Liu, L., Deng, H., Zhang, W., Madbouly, S. A., He, Z. et al. (2020). Novel internal emulsifiers for high biocontent sustainable pressure sensitive adhesives. *ACS Sustainable Chemistry & Engineering, 9(1),* 147–157. DOI 10.1021/acssuschemeng.0c05936.
5. Wang, X., Liang, H., Jiang, J., Wang, Q., Luo, Y. et al. (2020). A cysteine derivative-enabled ultrafast thiol-ene reaction for scalable synthesis of a fully bio-based internal emulsifier for high-toughness waterborne polyurethanes. *Green Chemistry, 22(17),* 5722–5729. DOI 10.1039/D0GC02213F.
6. Wang, L., Xiang, J., Wang, S., Sun, Z., Wen, J. et al. (2022). Synthesis of oleic-based primary glycol with high molecular weight for bio-based waterborne polyurethane. *Industrial Crops and Products, 176,* 114276. DOI 10.1016/j.indcrop.2021.114276.
7. Omrani, I., Babanejad, N., Shendi, H. K., Nabid, M. R. (2017). Preparation and evaluation of a novel sunflower oil-based waterborne polyurethane nanoparticles for sustained delivery of hydrophobic drug. *European Journal of Lipid Science and Technology, 119(8),* 1600283. DOI 10.1002/ejlt.201600283.
8. Fu, C., Zheng, Z., Yang, Z., Chen, Y., Shen, L. (2014). A fully bio-based waterborne polyurethane dispersion from vegetable oils: From synthesis of precursors by thiol-ene reaction to study of final material. *Progress in Organic Coatings, 77(1),* 53–60. DOI 10.1016/j.porgcoat.2013.08.002.

9. Gurunathan, T., Arukula, R., Chung, J. S., Rao, C. R. K. (2016). Development of environmental friendly castor oil-based waterborne polyurethane dispersions with polyaniline. *Polymers for Advanced Technologies, 27(11),* 1535–1540. DOI 10.1002/pat.3797.
10. Zhi, L., Zhang, C., Liu, Z., Liu, T., Dou, X. et al. (2022). Flexible decorative wood veneer with high strength, wearability and moisture penetrability enabled by infiltrating castor oil-based waterborne polyurethanes. *Composites Part B: Engineering, 230(11),* 109502. DOI 10.1016/j.compositesb.2021.109502.
11. Liang, H., Lu, Q., Liu, M., Ou, R., Wang, Q. et al. (2020). UV absorption, anticorrosion, and long-term antibacterial performance of vegetable oil based cationic waterborne polyurethanes enabled by amino acids. *Chemical Engineering Journal, 421,* 127774. DOI 10.1016/j.cej.2020.127774.
12. Zhang, Y., Zhang, W., Deng, H., Zhang, W., Zhang, C. et al. (2020). Enhanced mechanical properties and functional performances of cationic waterborne polyurethanes enabled by different natural phenolic acids. *ACS Sustainable Chemistry & Engineering, 8(47),* 17447–17457. DOI 10.1021/acssuschemeng.0c05883.
13. Hays, K. A., Ruther, R. E., Kukay, A. J., Cao, P., Saito, T. et al. (2018). What makes lithium substituted polyacrylic acid a better binder than polyacrylic acid for silicon-graphite composite anodes? *Journal of Power Sources, 384,* 136–144. DOI 10.1016/j.jpowsour.2018.02.085.
14. Li, A., Jia, Y., Sun, S., Xu, Y., Minsky, B. B. et al. (2018). Mineral-enhanced polyacrylic acid hydrogel as an oyster-inspired organic-inorganic hybrid adhesive. *ACS Applied Materials & Interfaces, 10(12),* 10471–10479. DOI 10.1021/acsami.8b01082.
15. Liu, N., Zhao, Y., Kang, M., Wang, J., Wang, X. et al. (2015). The effects of the molecular weight and structure of polycarbonatediols on the properties of waterborne polyurethanes. *Progress in Organic Coatings, 82,* 46–56. DOI 10.1016/j.porgcoat.2015.01.015.
16. Zhao, G., Ding, C., Pan, M., Zhai, S. (2018). Fabrication of NCC-SiO_2 hybrid colloids and its application on waterborne poly(acrylic acid) coatings. *Progress in Organic Coatings, 122,* 88–95. DOI 10.1016/j.porgcoat.2018.05.014.
17. Zhang, C., Liang, H., Liang, D., Lin, Z., Chen, Q. et al. (2021). Renewable castor-oil-based waterborne polyurethane networks: Simultaneously showing high strength, self-healing, processability and tunable multishape memory. *Angewandte Chemie International Edition in English, 60(8),* 4289–4299. DOI 10.1002/anie.202014299.
18. Wang, J., Lin, S., Wang, Y., Ma, M., Hu, C. (2019). Bi-functional water-born polyurethane-potassium poly(acrylate) designed for carbon-based electrodes of quasi solid-state supercapacitors: Establishing ionic tunnels and acting as a binder. *Journal of Power Sources, 413(21),* 77–85. DOI 10.1016/j.jpowsour.2018.12.028.
19. Wang, B., Wu, Z., Zhang, D., Wang, R., Song, P. et al. (2018). Antibacterial silicylacrylate copolymer emulsion for antifouling coatings. *Progress in Organic Coatings, 118(11),* 122–128. DOI 10.1016/j.porgcoat.2018.01.025.
20. Zhang, W., Zhang, Y., Liang, H., Liang, D., Zhang, C. et al. (2019). High bio-content castor oil based waterborne polyurethane/sodium lignosulfonate composites for environmental friendly UV absorption application. *Industrial Crops and Products, 142,* 111836. DOI 10.1016/j.indcrop.2019.111836.
21. Abdel-Wakil, W. S., Kamoun, E. A., Fahmy, A., Hassan, W., Abdelhai, F. et al. (2019). Assessment of vinyl acetate polyurethane-based graft terpolymers for emulsion coatings: Synthesis and characterization. *Journal of Macromolecular Science, Part A, 57(4),* 229–243. DOI 10.1080/10601325.2019.1691448.
22. Zhang, Y. Q., Björk, J., Weber, P., Hellwig, R., Diller, K. et al. (2015). Unusual deprotonated alkynyl hydrogen bonding in metal-supported hydrocarbon assembly. *Journal of Physical Chemistry C, 119(17),* 9669–9679. DOI 10.1021/acs.jpcc.5b02955.
23. Mondal, S., Hu, J. L. (2006). Structural characterization and mass transfer properties of nonporous segmented polyurethane membrane: Influence of hydrophilic and carboxylic group. *Journal of Membrane Science, 274(1–2),* 219–226. DOI 10.1016/j.memsci.2005.08.016.
24. Zhang, C., Hu, J., Chen, S., Ji, F. (2010). Theoretical study of hydrogen bonding interactions on MDI-based polyurethane. *Journal of Molecular Modeling, 16(8),* 1391–1399. DOI 10.1007/s00894-010-0645-4.

25. Liang, H., Li, Y., Huang, S., Huang, K., Zeng, X. et al. (2019). Tailoring the performance of vegetable oil-based waterborne polyurethanes through incorporation of rigid cyclic rings into soft polymer networks. *ACS Sustainable Chemistry & Engineering, 8(2),* 914–925. DOI 10.1021/acssuschemeng.9b05477.
26. Gok, M. K., Demir, K., Cevher, E., Ozsoy, Y., Cirit, U. et al. (2017). The effects of the thiolation with thioglycolic acid and l-cysteine on the mucoadhesion properties of the starch-graft-poly(acrylic acid). *Carbohydrate Polymers, 163(2),* 129–136. DOI 10.1016/j.carbpol.2017.01.065.
27. Zhu, H., Chen, Z., Sheng, Y., Luong Thi, T. T. (2010). Flaky polyacrylic acid/aluminium composite particles prepared using in-situ polymerization. *Dyes and Pigments, 86(2),* 155–160. DOI 10.1016/j.dyepig.2009.12.012.
28. Zheng, M., Cai, X., Tan, Y., Wang, W., Wang, D. et al. (2020). A high-resilience and conductive composite binder for lithium-sulfur batteries. *Chemical Engineering Journal, 389,* 124404. DOI 10.1016/j.cej.2020.124404.
29. Liu, X., Wu, J., Qiao, K., Liu, G., Wang, Z. et al. (2022). Topoarchitected polymer networks expand the space of material properties. *Nature Communications, 13(1),* 1622. DOI 10.1038/s41467-022-29245-0.
30. Xu, H., Xie, X. M. (2021). Super-tough and rapidly self-recoverable multi-bond network hydrogels facilitated by 2-ureido-4[1H]-pyrimidone dimers. *Chinese Chemical Letters, 32(1),* 521–524. DOI 10.1016/j.cclet.2020.04.039.
31. Li, Z., Zhu, Y. L., Niu, W., Yang, X., Jiang, Z. et al. (2021). Healable and recyclable elastomers with record-high mechanical robustness, unprecedented crack tolerance, and superhigh elastic restorability. *Advanced Materials, 33(27),* 2101498. DOI 10.1002/adma.202101498.
32. Hu, J., Peng, K., Guo, J., Shan, D., Kim, G. B. et al. (2016). Click cross-linking-improved waterborne polymers for environment-friendly coatings and adhesives. *ACS Applied Materials & Interfaces, 8(27),* 17499–17510. DOI 10.1021/acsami.6b02131.
33. Hu, X., Ding, Y., Liu, J., Deng, Y., Cheng, C. (2016). Synthesis and fluorescence properties of a waterborne polyurethane-acrylic hybrid polymeric dye. *Polymer Bulletin, 74(2),* 555–569. DOI 10.1007/s00289-016-1729-9.
34. Cakić, S. M., Valcic, M. D., Ristić, I. S., Radusin, T., Cvetinov, M. J. et al. (2019). Waterborne polyurethane-silica nanocomposite adhesives based on castor oil-recycled polyols: Effects of (3-aminopropyl) triethoxysilane (APTES) content on properties. *International Journal of Adhesion and Adhesives, 90(5),* 22–31. DOI 10.1016/j.ijadhadh.2019.01.005.
35. Anirudhan, T. S., Tharun, A. R. (2012). Preparation and adsorption properties of a novel interpenetrating polymer network (IPN) containing carboxyl groups for basic dye from aqueous media. *Chemical Engineering Journal, 181–182,* 761–769. DOI 10.1016/j.cej.2011.11.077.
36. Sirajudheen, P., Poovathumkuzhi, N. C., Vigneshwaran, S., Chelaveettil, B. M., Meenakshi, S. (2021). Applications of chitin and chitosan based biomaterials for the adsorptive removal of textile dyes from water–A comprehensive review. *Carbohydrate Polymers, 273,* 118604. DOI 10.1016/j.carbpol.2021.118604.
37. Liang, H., Liu, L., Lu, J., Chen, M., Zhang, C. (2018). Castor oil-based cationic waterborne polyurethane dispersions: Storage stability, thermo-physical properties and antibacterial properties. *Industrial Crops and Products, 117,* 169–178. DOI 10.1016/j.indcrop.2018.02.084.